Communications in Physics, Vol. 31, No. 4 (2021), pp. 425-438
DOI:https://doi.org/10.15625/0868-3166/16002

ELASTIC AND INELASTIC ALPHA TRANSFER IN THE ^{16}O+^{12}C SCATTERING

NGUYEN TRI TOAN PHUC[1,2,3], NGUYEN HOANG PHUC[3] †AND DAO TIEN KHOA[3]

[1]*Department of Nuclear Physics, Faculty of Physics and Engineering Physics, University of Science, Ho Chi Minh City, Vietnam*

[2]*Vietnam National University, Ho Chi Minh City, Vietnam*

[3]*Institute for Nuclear Science and Technology, VINATOM 179 Hoang Quoc Viet, Cau Giay, Hanoi, Vietnam*

E-mail: †nguyenhoangphuc.phy@gmail.com

Received 12 April 2021
Accepted for publication 5 May 2021
Published 26 October 2021

Abstract. *The elastic scattering cross section measured at energies $E \lesssim 10$ MeV/nucleon for some light heavy-ion systems having two identical cores like $^{16}O+^{12}C$ exhibits an enhanced oscillatory pattern at the backward angles. Such a pattern is known to be due to the transfer of the valence nucleon or cluster between the two identical cores. In particular, the elastic α transfer has been shown to originate directly from the core-exchange symmetry in the elastic $^{16}O+^{12}C$ scattering. Given the strong transition strength of the 2_1^+ state of ^{12}C and its large overlap with the ^{16}O ground state, it is natural to expect a similar α transfer process (or inelastic α transfer) to take place in the inelastic $^{16}O+^{12}C$ scattering. The present work provides a realistic coupled channel description of the α transfer in the inelastic $^{16}O+^{12}C$ scattering at low energies. Based on the results of the 4 coupled reaction-channels calculation, we show a significant contribution of the α transfer to the inelastic $^{16}O+^{12}C$ scattering cross section at the backward angles. These results suggest that the explicit coupling to the α transfer channels is crucial in the studies of the elastic and inelastic scattering of a nucleus-nucleus system with the core-exchange symmetry.*

Keywords: optical potential, coupled reaction channels, inelastic α transfer.

Classification numbers: 25.70.Hi, 21.60.Cs, 24.10.Eq.

I. INTRODUCTION

For some light nucleus-nucleus systems having two identical cores, the measured elastic scattering cross section shows an enhanced oscillation at backward angles. Such a pattern is established to be due to the elastic transfer of the valence nucleon or cluster between the two identical cores, and the observed oscillations originate from the interference between the elastic scattering and transfer amplitudes. The elastic transfer process was observed for several light heavy-ion (HI) systems at low energies [1], and it had been studied over the years to extract the structure information on the nucleon- and cluster spectroscopic factors (see, e.g., the review [2]) and the asymptotic normalization coefficients [3, 4]. Our recent studies have shown clearly the direct link between the elastic transfer process and the parity dependence of the nucleus-nucleus optical potential (OP), a natural consequence of the core-exchange symmetry of the dinuclear system under study [5, 6]. These results are an important step toward a deeper understanding of the core-exchange effect in the elastic nucleus-nucleus scattering, which has motivated a renewed interest on this topic [7].

The core-exchange symmetry and the associated transfer processes show up not only in the elastic scattering but also in the inelastic light HI scattering [2], which is dubbed as the inelastic transfer process. Although several experimental [8–18] and theoretical studies [19–22] were done to investigate the inelastic nucleon transfer, the inelastic α transfer process was rarely studied so far. The finite-range distorted wave Born approximation (DWBA) and, more recently, coupled reaction channels (CRC) method have been used to explore the impact of the inelastic α transfer on the ^{16}O+^{12}C [23–25], ^{9}Be+^{13}C [26], ^{16}O+^{20}Ne, and ^{14}N+^{10}B scattering at low energies [27]. These studies show a significant contribution of the α transfer process to the inelastic scattering cross section at the backward angles, a situation similar to that of the elastic α transfer. At variance with the elastic transfer, the inelastic α transfer carries more structure information on the core excitation, in particular, the α-core configuration of the excited state. A consistent CRC description of both the elastic and inelastic scattering with the explicit coupling to the elastic and inelastic α transfer channels must be a severe test of the models of the nucleus-nucleus OP, inelastic scattering- and transfer form factor (FF). Moreover, the α transfer channel seems to dominate over other transfer channels in some core-identical systems [28], so that to a good approximation the most important reaction channels belong to the same mass partition, and the number of unconstrained parameters can be reduced in the CRC calculation.

The α transfer in the elastic ^{16}O+^{12}C scattering at low energies is among the earliest elastic transfer reactions discovered [29], and this is also the most studied case of the elastic α transfer. The elastic ^{16}O+^{12}C scattering at energies $E \gtrsim 10$ MeV/nucleon is proven to be strongly refractive, with a pronounced nuclear rainbow pattern associated with a broad oscillation of the Airy minima observed in the elastic scattering cross section [30]. The observation of the nuclear rainbow also enabled an accurate determination of the real nucleus-nucleus OP down to small internuclear distances [31, 32]. In a recent study [28], we have carried out a systematic 10-channel CRC analysis of the elastic ^{16}O+^{12}C scattering at the refractive energies and shown that the enhanced oscillation of the elastic cross section at the backward angles is due to the multistep α transfer processes. In particular, the indirect α transfer through the 2^+_1 (4.44 MeV) excitation of ^{12}C was shown to be the dominant transfer process in the elastic ^{16}O+^{12}C scattering. Given a strong $E2$ coupling from the ground state to the 2^+_1 state of ^{12}C [33], the inelastic α transfer is expected to contribute

significantly to the inelastic ^{16}O+^{12}C scattering to the 2^+_1 state of ^{12}C at the backward angles. We note here a recent CRC analysis using the algebraic cluster model [25] that found some effects of the inelastic α transfer in the inelastic ^{16}O+^{12}C scattering data at $E_{\rm lab} = 80$ [24, 34, 35] and 84 MeV [24]. However, the inelastic couplings to the low-lying excited states of ^{12}C were found also strong at the backward angles, and the inelastic α transfer could not be determined unambiguously.

To further explore the α transfer contribution to the inelastic ^{16}O+^{12}C scattering, we perform in the present work a consistent CRC analysis of the elastic and inelastic ^{16}O+^{12}C scattering data measured at the energies $E_{\rm lab} = 100, 115.9$, and 124 MeV at the Strasbourg Tandem Vivitron [35–37]. These inelastic ^{16}O+^{12}C scattering data (for the 2^+_1 state of ^{12}C) were measured accurately up to the angles $\theta_{\rm c.m.}$ beyond 100°. At such large angles, the α transfer amplitude is well separated from the pure inelastic scattering amplitude [28] and can be unambiguously determined. Given the indirect α transfer via the 2^+_1 excitation of the ^{12}C core is the dominant process in the ^{16}O+^{12}C scattering [25, 28], we restrict our CRC coupling scheme to 4 reaction channels, with the ^{12}C core exchange in both the ground- and 2^+_1 states explicitly taken into account.

II. CRC FORMALISM

For the core-identical ^{16}O+^{12}C system, the elastic and inelastic α transfer channels are indistinguishable from the elastic and inelastic scattering channels, respectively. Therefore, the angular distributions of the observed elastic and inelastic ^{16}O+^{12}C scattering are the coherent sums of the pure scattering and α transfer amplitudes, and the total cross section is given by [2, 5]

$$\frac{d\sigma(\theta)}{d\Omega} = |f(\theta)|^2 = |f_{\rm scat}(\theta) + f_{\rm trans}(\pi - \theta)|^2 , \tag{1}$$

where the $f_{\rm scat}$ and $f_{\rm trans}$ are the pure scattering and α transfer amplitudes of the elastic or inelastic scattering. Historically, the elastic and inelastic scattering amplitudes were often evaluated separately first, and then added to the corresponding transfer amplitudes obtained in the DWBA (see, e.g., Refs. [21,24]). With the introducing of the CRC model [38,39], the simultaneous description of the involved scattering and transfer channels can be achieved in a consistent and unified manner.

We have performed recently a systematic CRC analysis of the elastic ^{16}O+^{12}C scattering at $E_{\rm lab} = 100 - 300$ MeV [28] taking into account up to 10 reaction channels between the ground state and excited states of the ^{12}C and ^{16}O nuclei, with the α transfer treated explicitly. In addition to the direct elastic α transfer between ^{12}C$_{\rm g.s.}$ and ^{16}O$_{\rm g.s.}$, we found a very strong contribution of the indirect α transfer via the 2^+_1 excitation of ^{12}C to the total elastic α transfer, and these two processes account mostly for the elastic α transfer cross section at the backward angles. This conclusion was confirmed by a later CRC study of the ^{16}O+^{12}C scattering at lower energies [25]. Given the dominance of the elastic scattering and inelastic scattering to the 2^+_1 state of ^{12}C, we restrict the present CRC calculation of the ^{16}O+^{12}C scattering to the 4-channel coupling scheme shown in Fig. 1, which is the smallest model space needed to describe simultaneously the elastic and inelastic ^{16}O+^{12}C scattering, with the α transfer explicitly taken into account.

In the CRC formalism, the coupled channel equation in the post form for a specific channel β is given by [38, 39]

$$(E_\beta - T_\beta - U_\beta)\chi_\beta = \sum_{\beta' \neq \beta, x = x'} \langle \beta | V | \beta' \rangle \chi_{\beta'} + \sum_{\beta' \neq \beta, x \neq x'} [\langle \beta | W_{\beta'} | \beta' \rangle + \langle \beta | \beta' \rangle (T_{\beta'} + U_{\beta'} - E_{\beta'})] \chi_{\beta'}, \tag{2}$$

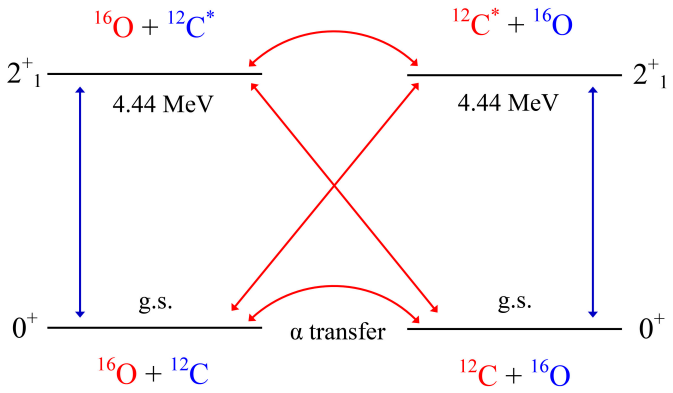

Fig. 1. 4-channel coupling scheme of the CRC calculation of the elastic ^{16}O+^{12}C scattering that includes both the direct and indirect (via the 2^+_1 excitation of the ^{12}C core) α transfers.

where β' indicates a channel different from β, x and x' are the mass partitions associated with the scattering and α-transfer channels. $E_{\rm i}$ and $T_{\rm i}$ are the asymptotic kinetic energy and kinetic energy operator of i-th channel in the centre-of-mass frame, respectively. U_β and $U_{\beta'}$ are the (diagonal) OP, and χ_β and $\chi_{\beta'}$ are the corresponding relative-motion wave functions of the dinuclear system. V is the local interaction operator and its matrix element $\langle\beta|V|\beta'\rangle$ is referred to as the form factor (FF). Due to the indistinguishability of the entrance and exit channels, the post- and prior forms of the coupled channel equation are the same, and the transition potential W_β is determined [38, 39] by

$$W_\beta = V_{\alpha+^{12}\rm C} + (U_{^{12}\rm C+^{12}\rm C} - U_{^{16}\rm O+^{12}\rm C}), \tag{3}$$

with the complex remnant term $(U_{^{12}\rm C+^{12}\rm C} - U_{^{16}\rm O+^{12}\rm C})$ determined by the difference between the OP of the exit channel and the that between the two cores. $V_{\alpha+^{12}\rm C}$ is the potential binding the α cluster to the ^{12}C core in ^{16}O. The CRC equations (2) for the 4 coupled reaction channels are solved iteratively using the code FRESCO written by Thompson [40], with the non-orthogonality corrections and finite-range complex remnant terms properly taken into account. All the OP's have their real part calculated in the double-folding model (DFM) [30] and the imaginary part parametrized in the Woods-Saxon (WS) form, which has the following form at the internuclear distance R

$$U(R) = N_R U_{\rm F}(E,R) - \frac{iW_V}{1+\exp[(R-R_V)/a_V]} + V_{\rm C}(R). \tag{4}$$

The Coulomb potential $V_{\rm C}(R)$ is given by that of a point charge interacting with a uniform charge sphere [39] of the radius $R_{\rm ch} = 0.95\times(A_{\rm T}^{1/3}+A_{\rm P}^{1/3})$ (fm), where $A_{\rm T}$ and $A_{\rm P}$ are the target and projectile mass number, respectively. This choice of the Coulomb potential gives practically about the same result of the optical model calculation as that using the more sophisticated one in Ref. [41] for the elastic light HI scattering [38]. The real folded potential $U_{\rm F}(E,R)$ was calculated in the DFM using the CDM3Y3 density dependent NN interaction [42], with the rearrangement term properly taken into account [30]. The ground state densities of ^{12}C and ^{16}O used in the DFM calculation were taken as the Fermi distributions with parameters adjusted to reproduce the empirical

matter radii of these nuclei [43]. The renormalization factor N_R of the real folded potential and WS parameters of the imaginary potential were adjusted to the best description of both the elastic and inelastic data at the forward angles up to $\theta_{\rm c.m.} \approx 90^\circ$. The Airy minima observed in the elastic data were served as the important constraint for these parameters.

The (complex) inelastic scattering FF for the $^{12}\mathrm{C}_{\rm g.s.} \to ^{12}\mathrm{C}_{2_1^+}$ transition is also obtained in the DFM [44] using the same CDM3Y3 interaction [30] with a complex density dependence suggested in Ref. [33], and the nuclear transition densities given by the 3α resonating group method (RGM) [45]. The real part of the diagonal OP for the $U_{^{16}\mathrm{O}+^{12}\mathrm{C}(2_1^+)}$ system is obtained in the DFM calculation using the diagonal density of the 2_1^+ state taken from the RGM calculation, and the imaginary part is assumed to be the same as the ground state absorption.

The α-cluster structure of ^{16}O enters the CRC calculation via the overlap function [38], which is also known as the reduced-width amplitude [46]

$$\langle ^{12}\mathrm{C}|^{16}\mathrm{O}\rangle = A_{NL}(^{16}\mathrm{O},^{12}\mathrm{C})\Phi_{NL}(\boldsymbol{r}_{\alpha+^{12}\mathrm{C}}), \tag{5}$$

where A_{NL} is the spectroscopic amplitude and $\Phi_{NL}(\boldsymbol{r}_{\alpha+^{12}\mathrm{C}})$ is the relative-motion wave function of the α+^{12}C system. This wave function is generated by the binding potential $V_{\alpha+^{12}\mathrm{C}}$ chosen in the WS form. In the present work, we adopt the WS geometry with $R = 3.72$ fm and $a = 0.845$ fm, parameterized in Ref. [47] based on the results of the five-body (^{12}C plus 4 nucleons) calculation [48]. This five-body model is an extended version of the orthogonality condition model (OCM) of ^{16}O [49], which can describe accurately both the 0_1^+ ground state and 0_2^+ excited state of ^{16}O. The WS potential based on the five-body model [48] has been used to reproduce with good accuracy the α transfer reaction ^{12}C(^{6}Li,d)^{16}O data at forward angles [47].

Using the fixed WS geometry [47], the depth of the binding potential $V_{\alpha+^{12}\mathrm{C}}$ for $\Phi_{NL}(\boldsymbol{r}_{\alpha+^{12}\mathrm{C}})$ is adjusted to reproduce the α separation energies of ^{16}O, with the ^{12}C core being in both the 0_1^+ ground state and 2_1^+ excited state

$$E_\alpha = E_\alpha(\mathrm{g.s.}) + E(^{12}\mathrm{C}^*), \tag{6}$$

where the α separation energy of ^{16}O in the ground state is $E_\alpha(\mathrm{g.s.}) \approx 7.162$ MeV [50], and $E(^{12}\mathrm{C}^*) \approx 4.44$ MeV is the excitation energy $E_{2_1^+}$ of ^{12}C. In Eq. (5), the relative-motion wave function $\Phi_{NL}(\boldsymbol{r}_{\alpha+^{12}\mathrm{C}})$ is characterized by the number of radial nodes N and cluster orbital angular momentum L that obey the Wildermuth's condition [38, 39]

$$2(N-1)+L = \sum_{i=1}^{4} 2(n_i-1)+l_i, \tag{7}$$

where l_i and n_i are, respectively, the orbital angular momentum and principal quantum number of each constituent nucleon in the α cluster. Here we use the number-of-nodes convention where the node at origin is included and the one at infinity is excluded.

Similar to our previous CRC analysis [28], the α spectroscopic factors $S_\alpha = |A_{NL}|^2$ are taken from the results of the cluster-nucleon configuration interacting model [51, 52]. This large-scale shell model calculation is carried out in the unrestricted *psd* model space and adopts an improved definition of S_α by Fliessbach [53, 54]. Although such a definition of S_α (also known as the amount of clustering) was used in microscopic cluster decay studies in the late nineties [55], it has been used in the CRC study of the direct α transfer reaction only recently [28]. A good

agreement between the CRC results obtained in Ref. [28] with the experimental data can serve as the validation for the use of this new S_α definition in other studies of the direct nuclear reactions.

The use of the WS shape of the α binding potential and spectroscopic factors based on the reliable structure models reduces the uncertainty associated with the α-cluster structure of ^{16}O. For the ground state of ^{16}O, we have $S_\alpha \approx 0.794$, $N = 3$, and $L = 0$ for the $\alpha + {}^{12}\mathrm{C}_{\mathrm{g.s.}}$ configuration, and $S^*_\alpha \approx 3.9$, $N = 2$, and $L = 2$ for $\alpha + {}^{12}\mathrm{C}_{2^+_1}$. The S^*_α adopted for the $\alpha + {}^{12}\mathrm{C}_{2^+_1}$ configuration is nearly 5 times large than that adopted for the $\alpha + {}^{12}\mathrm{C}_{\mathrm{g.s.}}$ configuration, which is due mainly to the M-substate degeneracy [56]. The ratio $S^*_\alpha/S_\alpha \approx 5$ is consistent with the results of different structure models as discussed in Ref. [28]. We note that the value $S^*_\alpha \approx 3.9$ calculated by the shell model [51, 52] for core-excited configuration is larger than those reported in the literature (see, e.g, Ref. [28]). This is a direct consequence of the Fliessbach's definition of α spectroscopic factors [53,54] used in Ref. [51,52], which properly takes into account the orthonormalization and antisymmetrization for the clustering channel.

III. ELASTIC AND INELASTIC ^{16}O+^{12}C SCATTERING WITH ALPHA TRANSFER

Given the significant α spectroscopic factors of the $\alpha + {}^{12}$C configurations of the ^{16}O nucleus discussed above and strong coupling effect of the α-cluster states shown by the structure calculations [57–60], some contributions of the α transfer channels to the elastic ^{16}O+^{12}C cross section are naturally expected at backward angles. A realistic description of the purely elastic scattering is very important for the present CRC study of the α transfer in the ^{16}O+^{12}C scattering. We consider here the elastic ^{16}O+^{12}C scattering data measured accurately at the energies $E_{\mathrm{lab}} = 100, 115.9$, and 124 MeV by the Strasbourg group [36], approaching the range of refractive energies for the ^{16}O+^{12}C system [30]. The refractive nature of the elastic ^{16}O+^{12}C scattering [30]

Table 1. Parameters (4) of the complex OP used in the 4-channel CRC calculation of the elastic and inelastic ^{16}O+^{12}C scatterings at $E_{\mathrm{lab}} = 100, 115.9$, and 124 MeV. N_R is the renormalization factor of the real folded OP, J_R and J_W are the volume integrals of the real and imaginary parts of the OP, respectively. σ_R is the total reaction cross section.

E_{lab} (MeV)	N_R	J_R (MeV fm^3)	W_V (MeV)	R_V (fm)	a_V (fm)	J_W (MeV fm^3)	σ_R (mb)
100	0.943	311.3	11.48	5.67	0.47	48.6	1305
115.9	0.950	311.7	12.80	5.70	0.46	55.0	1328
124	0.950	310.8	12.84	5.64	0.58	55.4	1410

is very well illustrated by the near-far decomposition of the elastic scattering amplitude based on the method developed by Fuller [61]. Namely, by decomposing the scattering amplitude into those representing the two waves traveling in θ that are running in the opposite directions around the scattering center, the elastic amplitude $f(\theta)$ can be determined as a sum of the near-side (f_{N}) and far-side (f_{F}) amplitudes

$$f(\theta) = f_{\mathrm{N}}(\theta) + f_{\mathrm{F}}(\theta). \tag{8}$$

The explicit expressions of these two amplitudes are discussed, e.g., in Refs. [28, 32]. We emphasize here that $f_{\mathrm{N}}(\theta)$ represents the waves deflected to the direction of θ on the near side of the scattering center, and the waves traveling on the opposite, far side of the scattering center to the

same angle θ give rise to $f_{\rm F}(\theta)$. Therefore, the *diffractive* near-side scattering occurs mainly at the surface of the two colliding nuclei, while the *refractive* far-side scattering penetrates more into the interior of the nucleus-nucleus system. The broad oscillation of the far-side cross section is well established [32] as the Airy oscillation of the nuclear rainbow pattern. The coupled channel (CC) description of the purely elastic ^{16}O+^{12}C scattering, *without* coupling to the α transfer channels, is shown in Fig. 2 where the cross section of the far-side scattering (8) has been obtained with 2 different absorption strengths of the complex OP from Table 1. One can see in Fig. 2 that the

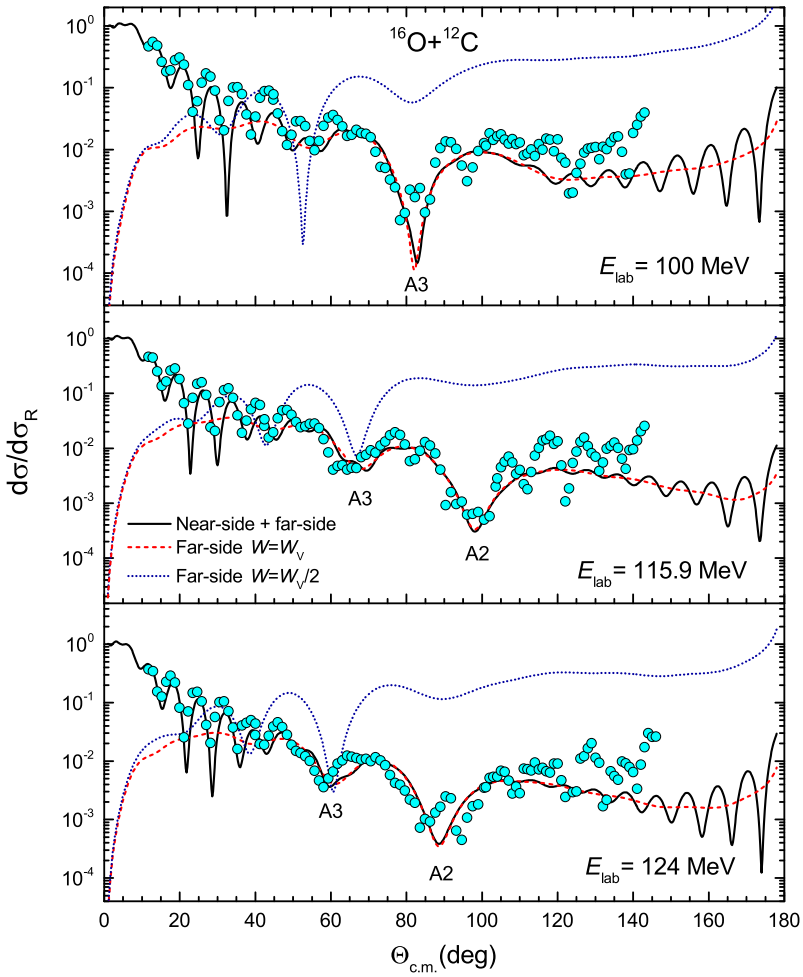

Fig. 2. CC description (solid lines) of the purely elastic ^{16}O+^{12}C scattering in comparison with the data measured at $E_{\rm lab} = 100, 115.9$, and 124 MeV [36]. The cross section of the far-side scattering has been obtained with 2 different strengths of the absorption (see parameters of the WS imaginary OP in Table 1) using the Fuller's method [61].

diffractive Fraunhofer oscillations at forward angles are followed immediately by a broad Airy oscillation of the elastic scattering cross section that is dominated by the far-side scattering. The

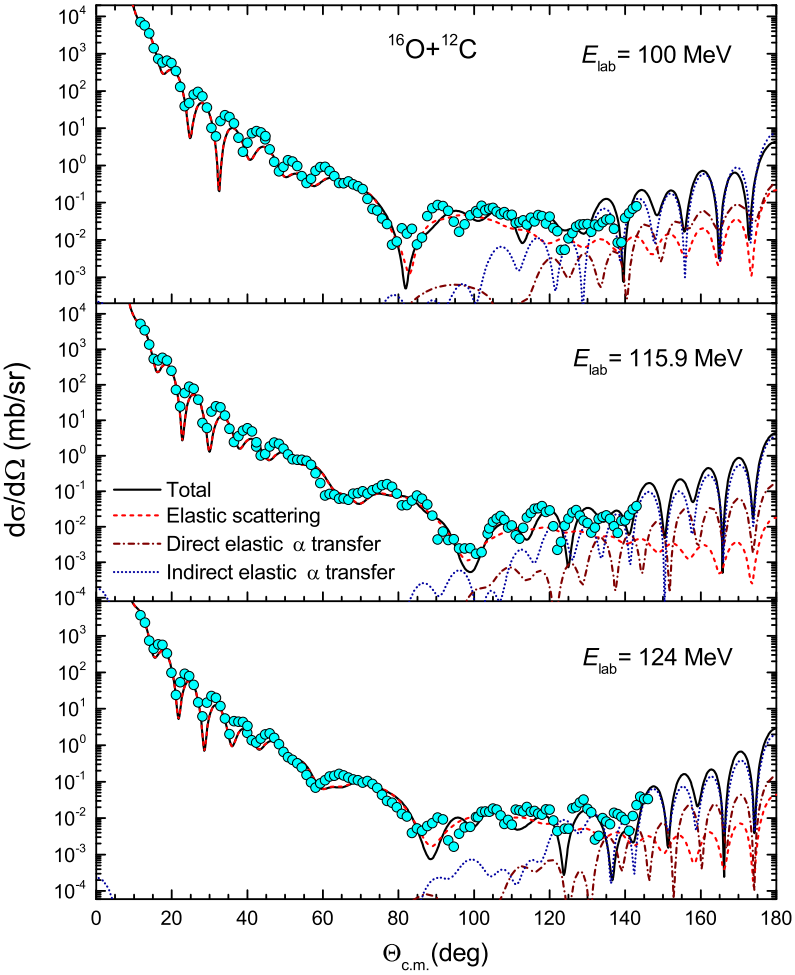

Fig. 3. 4-channel CRC description (solid lines) of the elastic ^{16}O+^{12}C data measured at $E_{\rm lab} = 100, 115.9$, and 124 MeV [36] including the direct and indirect elastic α transfer channels. The same complex OP (see Table 1) was used in the CRC calculation of the purely elastic scattering (dashed lines), direct α transfer (dash-dotted lines), and indirect α transfer via the 2^+_1 excited state of ^{12}C (dotted lines).

deep minima of the elastic ^{16}O+^{12}C scattering cross section observed in these data were established [28, 30] as the third Airy minimum (A3) at $\theta_{\rm c.m.} \approx 82^\circ$ in the energy of 100 MeV, and the second Airy minimum (A2) at $\theta_{\rm c.m.} \approx 98^\circ$ and 88° in the energies of 115.9 and 124 MeV, respectively. The renormalization factor N_R of the real folded OP and WS parameters of the imaginary OP in Table 1 were fine tuned to reproduce both the Fraunhofer diffraction at forward angles and the broad Airy oscillation at medium and large angles, up to $\theta_{\rm c.m.} \approx 100^\circ$. Since the coupling scheme considered in this work (Fig. 1) is different from those in Ref. [28], a reproduction of experimental data requires different amounts of effective contributions from channels not explicitly

included in the model space. Consequently, the fitted OP parameters from the two works have slightly different values to account for these scheme-specific contributions.

Figure 2 also illustrates that while the elastic data at forward angles are well described as the purely elastic scattering, the quick oscillation of the measured elastic scattering cross section at medium and large angles cannot be reproduced by the CC calculation in this work or the optical model (OM) description in Ref. [28]. Moreover, the leading-order Airy minima (A1 and A2) predicted by the OM analysis [30] at $\theta_{\rm c.m.} > 100^\circ$ are strongly deteriorated due to the contribution of the elastic α transfer in this angular range [6].

The results of the 4-channel CRC calculation of the elastic ^{16}O+^{12}C scattering with the α transfer channels being included are shown in Fig. 3, and one can see clearly the contribution of the elastic α transfer to the total elastic cross section at backward angles. The contribution of the indirect (two-step) elastic α transfer via the 2_1^+ state of ^{12}C is much stronger than the direct elastic α transfer one and dominates the elastic cross section at the most backward angles. This is due to a large spectroscopic factor S_α of the $\alpha + {}^{12}\mathrm{C}^*_{2_1^+}$ configuration of the ^{16}O nucleus discussed above. We reiterate that our CRC calculation does not treat the S_α factors as free parameters but adopts the S_α values predicted by the large-scale shell model calculation [51, 52]. The CRC results also show that the elastic α transfer occurring in the elastic ^{16}O+^{12}C cross section at backward angles is well separated from the purely elastic scattering at the considered energies. The situation is different at lower energies [25] where the cross section of the purely elastic scattering is slightly larger and not as clearly distinct from that of the elastic α transfer at backward angles.

The higher the incident energy the more elastic α transfer is separated from the elastic scattering at medium and large angles, and this effect is more pronounced [28] in the elastic ^{16}O+^{12}C data at $E_{\rm lab} = 300$ MeV. Within the semiclassical interpretation of the elastic HI scattering [38], more nonelastic channels are open with the increasing energy, and the absorption becomes, therefore, stronger and reduces the elastic flux at small partial waves, leading to a rapid decrease of the elastic scattering cross section at medium and large angles. A similar effect can be seen also in the cross section of the elastic α transfer. Because the elastic transfer amplitude at $\pi - \theta$ is added (1) to the elastic scattering amplitude at θ, the elastic α transfer occurring mainly at the surface of the two colliding nuclei (or at forward angles) has the cross section largest at backward angles. We have further performed the near-far decomposition (8) of the total CRC elastic ^{16}O+^{12}C amplitude at the considered energies and the results are shown in Fig. 4. Because of the surface character of the α transfer, the near-side cross section is naturally enhanced at large angles when the CRC coupling to the α transfer channels is included. It is interesting that a stronger near-side cross section given by the elastic α transfer amplitude at angles $\pi - \theta$ turns out to have a broad Airy-like oscillation from large to medium angles, which is likely associated with the (far-side) refracted α transfer waves evaluated at angles θ. In conclusion, the observed oscillating distortion of the smooth Airy pattern of the nuclear rainbow in the elastic ^{16}O+^{12}C scattering [6] is due mainly to a stronger interference of the near-side and far-side scattering waves at medium and large angles caused by the (direct and indirect) elastic α transfer.

The CRC results obtained within the 4-channel coupling scheme shown in Fig. 1 describe well the data measured at the considered energies for the inelastic ^{16}O+^{12}C scattering to the 2_1^+ state of ^{12}C by Szilner *et al.* [35, 37] (see Fig. 5). The purely inelastic scattering cross section at forward angles has the well established diffractive pattern that can be properly reproduced by the CC calculation *without* coupling to the α transfer channels (dashed lines in Fig. 5). At variance

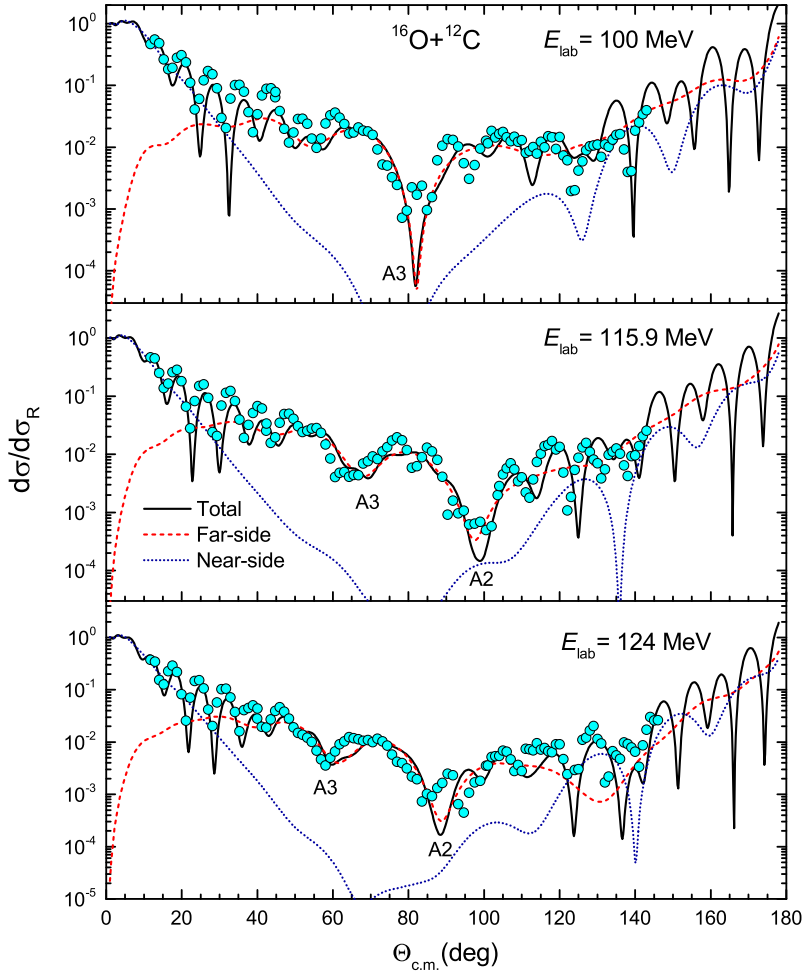

Fig. 4. Near-far decomposition (8) of the CRC elastic ^{16}O+^{12}C cross section at $E_{\rm lab} =$ 100, 115.9, and 124 MeV (solid lines) into the near-side (dotted lines) and far-side (dashed lines) scattering cross sections using the Fuller's method [61], in comparison with the measured data [36].

with the elastic ^{16}O+^{12}C scattering data where a pronounced rainbow pattern could be revealed at the three considered energies, a similar broad Airy oscillation cannot be seen in the inelastic ^{16}O+^{12}C scattering data for the 2_1^+ state of ^{12}C. Such a disappearance of the rainbow pattern in the inelastic ^{16}O+^{12}C scattering has been explained recently [62] by extending the Fuller's decomposition method (8) for the near-far decomposition of the inelastic scattering amplitude. It was shown that a destructive interference of the coupled partial waves of different multipoles can suppress the oscillating Airy pattern in the inelastic scattering cross section when the nuclear excitation has nonzero spin [62]. Such an effect is analogous to the opacity of an optical prism caused by the refraction of light rays having different wave lengths.

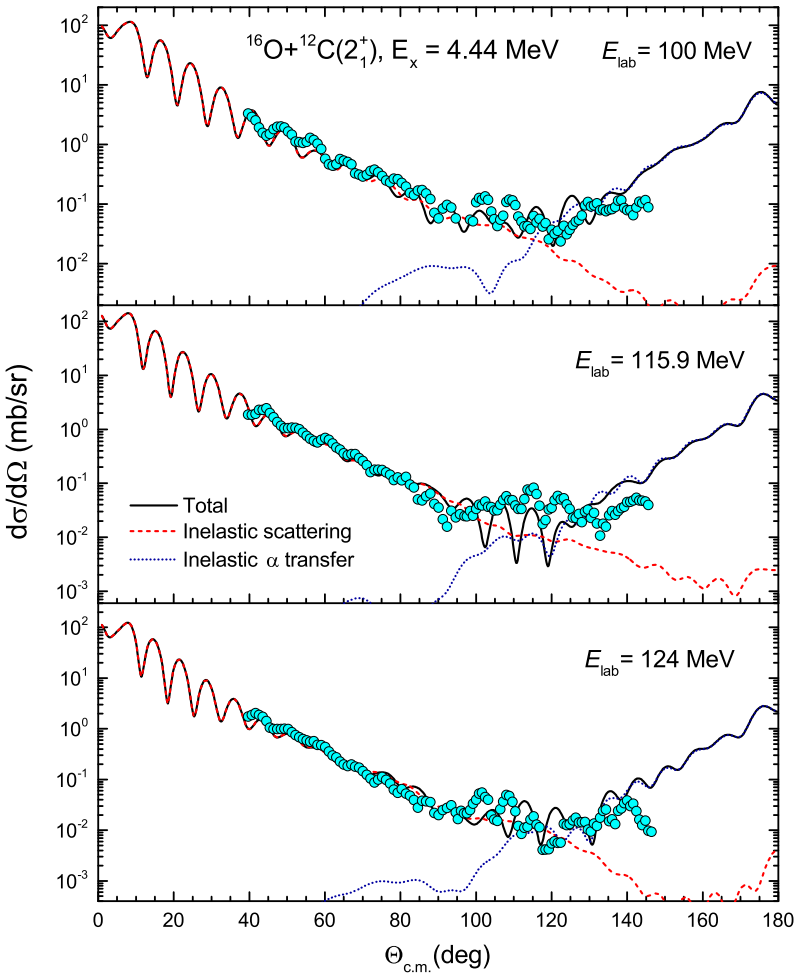

Fig. 5. CRC description (solid lines) of the inelastic ^{16}O+^{12}C scattering to the 2^+_1 state of ^{12}C in comparison with the data measured at $E_{\rm lab} = 100, 115.9$, and 124 MeV by Szilner *et al.* [35, 37]. The purely inelastic scattering (dashed lines) and inelastic α transfer (dotted lines) cross sections were obtained with the same OP as that used in the CRC calculation of the elastic ^{16}O+^{12}C scattering (Table 1).

Similar to the elastic ^{16}O+^{12}C scattering considered above, the rise of the inelastic scatetring cross section at large angles is overwhelmingly dominated by the inelastic α transfer in the ^{16}O+^{12}C system. A consistently good CRC description of both the elastic and inelastic ^{16}O+^{12}C scattering data measured at $E_{\rm lab} = 100, 115.9$, and 124 MeV [35, 37] has been obtained for the first time in the present work (see Figs. 3 and 5) with the large-angle data dominated by the elastic and inelastic α transfer. Like the elastic scattering case, the contribution of the inelastic α transfer to the inelastic scattering cross section becomes stronger with the increasing energies. At the considered energies, the inelastic α transfer contribution begins to dominate the inelastic scattering cross section at $\theta_{\rm c.m.} > 120^\circ$ resulting in a distinctive V-shape that cannot be properly described without

coupling to the α transfer channels. Thus, our CRC results suggest that the elastic and inelastic ^{16}O+^{12}C scattering data taken at higher incident energies of $E_{\rm lab} > 100$ MeV are a suitable probe of the α cluster structure of ^{16}O and ^{12}C that can be revealed in the elastic and inelastic α transfer processes.

IV. SUMMARY

The impact by the elastic and inelastic α transfer in the ^{16}O+^{12}C system on the elastic scattering and inelastic scattering to the 2^+_1 state of ^{12}C has been thoroughly studied in a consistent 4-channel CRC analysis of the elastic and inelastic ^{16}O+^{12}C scattering data measured at the incident energies of $E_{\rm lab} = 100, 115.9$, and 124 MeV. Our CRC calculations take explicitly into account the coupling between the elastic scattering, inelastic scattering, and α transfer channels, using the diagonal and transition ^{16}O+^{12}C and ^{12}C+^{12}C potentials obtained in the DFM calculation with the essential structure inputs like S_α, overlap function, and nuclear transition densities taken from the reliable structure models.

With the indirect α transfer via the 2^+_1 excitation of the ^{12}C core properly taken into account in the 4-channel CRC calculation of the elastic ^{16}O+^{12}C scattering, a consistently good description of both the elastic and inelastic ^{16}O+^{12}C data at the considered energies has been obtained for the first time. The contribution from the elastic and inelastic α transfer is found to be dominant in the elastic and inelastic scattering cross sections at backward angles. The α transfer cross section at the considered energies is well separated from the purely scattering cross section, at variance with that observed in the ^{16}O+^{12}C data at the lower energy $E_{\rm lab} \approx 80$ MeV [25]. Therefore, the results of the present CRC analysis suggest that the extensive elastic and inelastic ^{16}O+^{12}C scattering data at refractive energies of $E_{\rm lab} > 100$ MeV are more appropriate for the studies of elastic and inelastic α transfer.

ACKNOWLEDGMENTS

The present research was supported, in part, by the National Foundation for Scientific and Technological Development (NAFOSTED Project No. 103.04-2017.317). We thank Suzana Szilner for her helpful communication on the inelastic ^{16}O+^{12}C scattering data, and Alexander Volya for providing us with the α spectroscopic factors obtained from the large-scale shell-model calculation. The permission by Masayasu Kamimura to use the RGM nuclear transition densities in the present DFM calculation is also strongly appreciated.

REFERENCES

[1] P. Braun-Munzinger and J. Barrette, *Phys. Rep.* **87** (1982) 209.
[2] W. von Oertzen and H. Bohlen, *Physics Reports* **19** (1975) 1 .
[3] A. M. Mukhamedzhanov, H. L. Clark, C. A. Gagliardi, Y.-W. Lui, L. Trache, R. E. Tribble, H. M. Xu, X. G. Zhou, V. Burjan, J. Cejpek, V. Kroha and F. Carstoiu, *Phys. Rev. C* **56** (1997) 1302.
[4] R. E. Tribble, C. A. Bertulani, M. L. Cognata, A. M. Mukhamedzhanov and C. Spitaleri, *Rep. Prog. Phys.* **77** (2014) 106901.
[5] N. T. T. Phuc, R. S. Mackintosh, N. H. Phuc and D. T. Khoa, *Phys. Rev. C* **100** (2019) 054615.
[6] N. H. Phuc, D. T. Khoa and N. T. T. Phuc, *Eur. Phys. J. A* **57** (2021) 7.
[7] J. Dohet-Eraly and P. Descouvemont, *arXiv:2101.06942 [nucl-th]* (2021) .
[8] K. Potthast, H. Freiesleben, P. Rosenthal, B. Kamys, Z. Rudy, H. Paetz gen. Schieck and L. Sydow, *Nucl. Phys. A* **629** (1998) 656.

[9] J. Sromicki, M. Hugi, J. Lang, R. Müller, E. Ungricht, L. Jarczyk, B. Kamys, A. Magiera, Z. Rudy, A. Strzałkowski and B. Zebik, *Nucl. Phys. A* **406** (1983) 390.
[10] L. Jarczyk, B. Kamys, A. Magiera, A. Strzalkowski, S. Albergo, S. Costa, R. Potenza, J. Romanski, C. Tuvé, R. Barná, V. D'Amico, D. De Pasquale and G. Mannino, *Phys. Rev. C* **44** (1991) 2053.
[11] L. Jarczyk, B. Kamys, A. Magiera, Z. Rudy, A. Strzalkowski, B. Styczen, J. Hebenstreit, W. Oelert, P. von Rossen and H. Seyfarth, *Phys. Rev. C* **46** (1992) 1393.
[12] A. Rudchik, A. Budzanowski, V. Chernievsky, B. Czech, L. Głowacka, S. Kliczewski, A. Mokhnach, O. Momotyuk, S. Omelchuk, V. Pirnak, K. Rusek, R. Siudak, I. Skwirczyńska, A. Szczurek and L. Zemło, *Nucl. Phys. A* **695** (2001) 51.
[13] L. T. Chua, A. Gobbi, M. W. Sachs, D. Shapira, R. Wieland and D. A. Bromley, *Nuovo Cimento A* **47** (1978) 430.
[14] H. G. Bohlen, X. S. Chen, J. G. Cramer, P. FrÃ¶brich, B. Gebauer, H. Lettau, A. Miczaika, W. von Oertzen, R. Ulrich and T. Wilpert, *Z. Phys. A* **322** (1985) 241.
[15] H. Voit, N. Bischof, W. Tiereth, I. Weitzenfelder, W. von Oertzen and B. Imanishi, *Nucl. Phys. A* **476** (1988) 491.
[16] C. Gelbke, G. Baur, R. Bock, P. Braun-Munzinger, W. Grochulski, H. Harney and R. Stock, *Nucl. Phys. A* **219** (1974) 253.
[17] D. Kalinsky, D. Melnik, U. Smilansky, N. Trautner, B. Watson, Y. Horowitz, S. Mordechai, G. Baur and D. Pelte, *Nucl. Phys. A* **250** (1975) 364.
[18] W. von Oertzen, T. Wilpert, B. Bilwes, L. Stuttge, J. L. Ferrero, J. A. Ruiz, I. J. Thompson and B. Imanishi, *Z. Phys. A* **353** (1996) 373.
[19] B. Imanishi and W. von Oertzen, *Phys. Rep.* **155** (1987) 29 .
[20] B. Imanishi, V. Denisov and T. Motobayashi, *Phys. Rev. C* **55** (1997) 1946.
[21] G. Baur and H. Wolter, *Phys. Lett. B* **51** (1974) 205.
[22] J.-M. Sparenberg, D. Baye and B. Imanishi, *Phys. Rev. C* **61** (2000) 054610.
[23] R. DeVries, *Nucl. Phys. A* **212** (1973) 207.
[24] H. G. Bohlen, H. Ossenbrink, W. von Oertzen, P. Wust, H. Hafner and K. Wannebo, *Z. Phys. A* **285** (1978) 379.
[25] J. L. Ferreira, J. Lubian, R. Linares, M. J. Ermamatov, H. Yépez-Martínez and P. O. Hess, *Eur. Phys. J. A* **55** (2019) 94.
[26] A. Barbadoro, F. Pellegrini, G. F. Segato, L. Taffara, I. Gabrielli and M. Bruno, *Phys. Rev. C* **41** (1990) 2425.
[27] T. Motobayashi, I. Kohno, T. Ooi and S. Nakajima, *Nucl. Phys. A* **331** (1979) 193.
[28] N. T. T. Phuc, N. H. Phuc and D. T. Khoa, *Phys. Rev. C* **98** (2018) 024613.
[29] W. Von Oertzen, H. Gutbrod, M. Müller, U. Voos and R. Bock, *Phys. Lett. B* **26** (1968) 291 .
[30] D. T. Khoa, N. H. Phuc, D. T. Loan and B. M. Loc, *Phys. Rev. C* **94** (2016) 034612.
[31] M. Brandan and G. Satchler, *Phys. Rep.* **285** (1997) 143 .
[32] D. T. Khoa, W. von Oertzen, H. G. Bohlen and S. Ohkubo, *J. Phys. G* **34** (2007) R111.
[33] D. T. Khoa and D. C. Cuong, *Physics Letters B* **660** (2008) 331 .
[34] H. H. Gutbrod, R. Bock, W. von Oertzen and U. C. Schlotthauer-Voos, *Z. Phys.* **262** (1973) 377.
[35] S. Szilner, F. Haas, Z. Basrak, R. Freeman, A. Morsad and M. Nicoli, *Nuclear Physics A* **779** (2006) 21 .
[36] M. P. Nicoli, F. Haas, R. M. Freeman, S. Szilner, Z. Basrak, A. Morsad, G. R. Satchler and M. E. Brandan, *Phys. Rev. C* **61** (2000) 034609.
[37] S. Szilner, *et al*., IAEA Database EXFOR, http://www-nds.iaea.org/exfor/.
[38] G. Satchler, *Direct nuclear reactions*, Clarendon, Oxford, 1983.
[39] I. Thompson and F. Nunes, *Nuclear reactions for astrophysics*, Cambridge University Press, Cambridge, UK, 2009.
[40] I. J. Thompson, *Computer Physics Reports* **7** (1988) 167 .
[41] J. E. Poling, E. Norbeck and R. R. Carlson, *Phys. Rev. C* **13** (1976) 648.
[42] D. T. Khoa, G. R. Satchler and W. von Oertzen, *Phys. Rev. C* **56** (1997) 954.
[43] D. T. Khoa, *Phys. Rev. C* **63** (2001) 034007.
[44] D. T. Khoa and G. Satchler, *Nuclear Physics A* **668** (2000) 3 .
[45] M. Kamimura, *Nuclear Physics A* **351** (1981) 456 .
[46] H. Horiuchi, K. Ikeda and K. Katō, *Prog. Theo. Phys. Supp.* **192** (2012) 1.
[47] T. Fukui, Y. Kanada-En'yo, K. Ogata, T. Suhara and Y. Taniguchi, *Nucl. Phys. A* **983** (2019) 38 .
[48] W. Horiuchi and Y. Suzuki, *Phys. Rev. C* **89** (2014) 011304.

[49] Y. Suzuki, *Prog. Theor. Phys.* **55** (1976) 1751.
[50] D. Tilley, H. Weller and C. Cheves, *Nuclear Physics A* **564** (1993) 1 .
[51] A. Volya and Y. M. Tchuvil'sky, *Phys. Rev. C* **91** (2015) 044319.
[52] A. Volya, private communication (unpublished).
[53] T. Fliessbach and H. Mang, *Nuclear Physics A* **263** (1976) 75 .
[54] T. Fliessbach and P. Manakos, *J. Phys. G* **3** (1977) 643.
[55] R. Lovas, R. Liotta, A. Insolia, K. Varga and D. Delion, *Physics Reports* **294** (1998) 265 .
[56] M. Ichimura, A. Arima, E. Halbert and T. Terasawa, *Nuclear Physics A* **204** (1973) 225 .
[57] E. Epelbaum, H. Krebs, T. A. Lähde, D. Lee, U.-G. Meißner and G. Rupak, *Phys. Rev. Lett.* **112** (2014) 102501.
[58] R. Bijker and F. Iachello, *Phys. Rev. Lett.* **112** (2014) 152501.
[59] Y. Kanada-En'yo, *Phys. Rev. C* **96** (2017) 034306.
[60] X. Wang, G. Dong, Z. Gao, Y. Chen and C. Shen, *Phys. Lett. B* **790** (2019) 498.
[61] R. C. Fuller, *Phys. Rev. C* **12** (1975) 1561.
[62] N. H. Phuc, D. T. Khoa, N. T. T. Phuc and D. C. Cuong, *Eur. Phys. J. A* **57** (2021) 75.